Desalination and Water Treatment
www.deswater.com

doi: 10.1080/19443994.2015.1021841

57 (2016) 8575–8582
April

Taylor & Francis
Taylor & Francis Group

Optimization of arsenic removal from pyrite ash by NaOH leaching using central composite design

Tuğba Türk

Department of Mining Engineering, Karadeniz Technical University, Trabzon 61080, Turkey, Tel. +90 462 377 4064; Fax: +90 462 325 7405; email: tugbaturk@yahoo.com.tr

Received 14 April 2014; Accepted 15 February 2015

ABSTRACT

The objective of this study was to leach arsenic from pyrite ash waste under basic conditions with sodium hydroxide (NaOH) by optimizing the leaching process using response surface methodology (RSM). For optimization of this process, the central composite design (CCD), the most popular of the many classes of RSM designs, was employed. The effects of temperature, leaching time, and NaOH concentration on the leaching of arsenic were investigated. The arsenic leaching yield increased with increasing temperature. Unlike the temperature, the leaching time had a negligible effect on the yield. The arsenic leaching yield of pyrite ash waste was in the range of 67–93%. The optimum conditions identified for arsenic leaching from pyrite ash were as follows: NaOH concentration at 3 M, leaching temperature at 89˚C, and leaching time of 182 min. Under these conditions, an average leaching yield of 92.15% was achieved from pyrite ash. The results of this study showed that NaOH can be used as a potential extractant for the removal of arsenic from pyrite ash. The regression equation and analysis of variance were obtained using MINITAB. A model was obtained by means of variance analysis at 0.967 confidence level.

Keywords: Statistical modeling; Pyrite ash; Arsenic; Alkaline leaching

1. Introduction

A significant part of wastes are produced by mineral-working and metallurgical processes. The annual acid production capacity in Bandırma Sulfuric acid production factory is approximately 25,000 tons pure grade [1]. In Turkey, pyrite ash is obtained as a waste product from the roasting of pyrite ores used as a raw material during manufacturing process of sulfuric acid. These wastes are generally released into the environment or the sea [2]. Pyrite ash wastes are used in a variety of fields in order to prevent pollution and recycle waste products [1–4]. Since pyrite ash wastes consist of approximately 60–65% iron, they can be used as a raw blast furnace feed in iron production, but the ashes need to be converted into pellet form [5]. A recent study from Turkey intended to convert pyrite ashes into pellet form in order to bestow the appropriate characteristics for use in blast furnaces as iron ore [6]. In their study, Alp et al. [1] investigated the potential use of pyrite ash as an iron source in the production of Portland cement and demonstrated that pyrite ash can be used successfully as an iron source in cement production. In another study, Tuğrul et al. added calcium hydrate and calcium chloride to bentonite, employed as a binder in pelletization, to make it more efficient. Their results showed that pyrite ash can be agglomerated to pellets and used in the iron production industry as a blast furnace feed [3].

Pyrite ash may contain metals such as copper, zinc, and nickel, and these metals can be recycled using hydrometallurgical techniques [7,8]. Various physical and chemical tests are used to determine the potential impact of these wastes on the environment when stored in a disposal site. TCLP and SPLP tests of waste were performed to indirectly evaluate the release and mobility of contaminants to the surrounding environment by normal rain or acidic rain [9]. In a previous study, leachability tests were performed for the environmental characterization of the metallurgical wastes, including pyrite ash, and leaching concentrations of As and heavy metals were compared with their criteria. TCLP extraction results showed that the concentrations of As leached were below the limit. Considering SPLP test results, the release of As was found to be relatively high. It was observed that in terms of heavy metals, these wastes can be a source of potential contamination [1].

Arsenic, which is one of the most toxic pollutants, is discharged into the environment from industrial and mining wastes, metal smelting, agricultural fertilizers, and insecticides [10]. The dust material containing substances such as lead, zinc, copper, iron, arsenic can be treated by pyrometallurgical [11] or hydrometallurgical processes [11,12]. Metals containing arsenic need to be heated to about 500℃ in the pyrometallurgical industry. The oxygen flow is carefully controlled. This means that the resulting arsenic trioxide is first volatilized and subsequently recondensed [13]. However, the arsenic that is volatilized in this process may then represent a further cause of pollution. Moreover, solidification and stabilization are no longer regarded as "best practice" for toxic wastes with arsenic content [14]. Due to these disadvantages, the need for hydrometallurgical processes has now emerged in order to obtain metals from materials containing arsenic [12]. Hydrometallurgical processes, including pressure leaching, acid leaching, alkali leaching, solvent extraction, and flotation, have been used for As removal. The leaching of arsenic from arsenic-containing materials is usually performed under strong acidic or basic conditions [15]. However, the extraction method with basic reagent has been found to be more environment friendly, as compared to the acidic reagent. Ito et al. [16] recommended the use of NaOH and concluded that arsenic leaching from sludge was achieved at high pH. Experiments for arsenic from sewage sludge were carried out at pH of 1–11. Arsenic in the sludge was effectively eluted from the sludge by increasing the sludge pH. In this study, statistically designed experiments were performed to investigate the removal of arsenic from pyrite ash using NaOH.

2. Experimental design

2.1. The response surface methodology

Response surface methodology (RSM) consists of a series of mathematical and statistical techniques used to determine the relation between responses in experiments and independent variables [17]. The technique was first described by G.E.P. Box and K.B. Wilson in [18]. The literature contains a large number of studies in which RSM was applied in experimental design. RSM generally involves two main steps:

(1) Design and performance of experiments.
(2) Surface modeling with regression.

The basic aim in RSM is to determine optimum or acceptable study conditions and regions. RSM permits independent variables to be converted into a function. If a linear model is insufficient in accounting for experimental data, then factorial design types need to be employed. The most widely used design types in determining response functions are full factorial design, fractional factorial design, and center composite design (CCD) [16]. With its flexibility and a wide range of functions and forms, CCD provides successful results in estimating a response surface [17]. CCD is an experimental design technique with expanded center points that allows charts to be produced. Codes were set up for each factor: distance from center point was ±1 for factorial points, and $\pm\beta$ beyond factorial points for axial points (Table 1).

Experimental results obtained from the CCD model were described in the form as given in Eq. (1)

$$Y = \beta_0 + \sum_{i=1}^{k} \beta_i \chi_i + \sum_{i=1}^{k-1} \sum_{j=i+1}^{k} \beta_{ij} \chi_i \chi_j + \sum_{i=1}^{k} \beta_{ii} \chi_{i^2} \qquad (1)$$

Table 1
Relationship between coded and actual value of the variables

Code	Actual level of variable
$-\beta$	$x_{\min}$
−1	$[(x_{\max} + x_{\min})/2] - [(x_{\max} - x_{\min})/2\alpha]$
0	$(x_{\max} + x_{\min})/2$
+1	$[(x_{\max} + x_{\min})/2] + [(x_{\max} - x_{\min})/2\alpha]$
$+\beta$	$x_{\max}$

Note: $x_{\max}$ and $x_{\min}$ = maximum and minimum values of x, respectively; $\alpha = 2^{k/4}$; k = number of variables.

Table 2
Chemical composition of pyrite ash wastes

Component	%	Component	%	Component	ppm
SiO_2	8.13	Na_2O	0.09	As	802.5
Fe_2O_3	86.54	Cr_2O_3	0.005	Cu	9,481
Al_2O_3	1.63	P_2O_5	0.04	Pb	165
TiO_2	0.13	K_2O	0.13	Zn	1,134
CaO	0.59	BaO	0.03	Co	2,033
MgO	0.44	NiO	0.01	Mn	77.46
ZrO_2	0.01	SO_3	1.38	Sb	25.9

where y is the predicted response β_0, the constant coefficient β_i, the linear coefficient β_{ii}, the quadratic coefficient $\beta_{ij,}$ the interaction coefficient, and k, the number of factors [19,20]. Optimized leaching conditions were estimated using Design-Expert software's (version 9.0.3) numerical and graphical optimization tools.

3. Experimental

3.1. Material characterization

The samples of pyrite ash wastes were obtained from Bandırma Borax and Boric Acid Establishment, Turkey. The chemical compositions of the pyrite ash (Table 2) were identified using X-ray fluorescence techniques and ICP/OES & MS (ACME Anal. Lab.). As can be seen in Table 2, the pyrite ash sample contained significant levels of Fe_2O_3 (86.54%) and SiO_2 (8.13%), whereas the contents of other metal oxides were less than 10%. The most important hazardous oxides in the pyrite ash were ZnO, CuO, and PbO. Pyrite ash also contained metals such as As (802 ppm), which is potentially dangerous (Table 2). Particle size analysis of the sample conducted using laser diffraction method (Malvern Master Sizer) revealed that 80% of the sample was finer than 50 μm

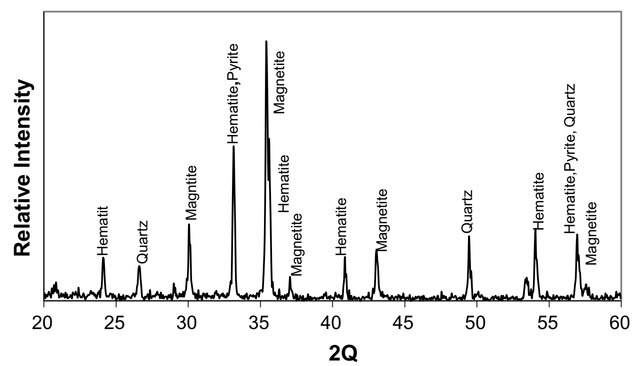

Fig. 2. Results of X-ray diffractogram of pyrite ash wastes.

Table 3
Parameters and their corresponding levels

Factors	Low level −1	Central level 0	High level +1
Temperature, ℃ (X_1)	70	80	90
NaOH concentration, M (X_2)	1	1.75	2.5
Reaction time, min. (X_3)	120	240	360

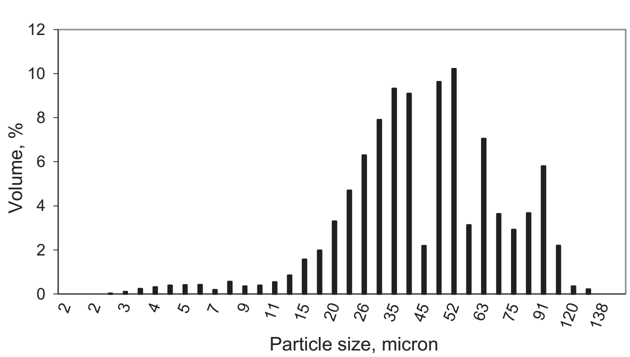

Fig. 1. Particle size distribution of the pyrite ash wastes.

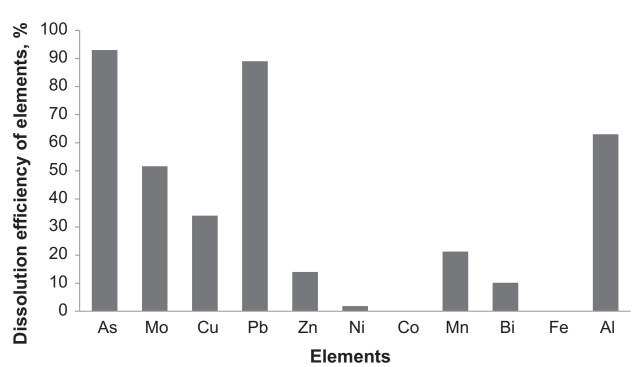

Fig. 3. Dissolution efficiency of elements.

(Fig. 1). The crystalline phase composition of the material was investigated using X-ray diffractometer (RIGAKU, D/Max-IIIC). The XRD pattern shown in Fig. 2 revealed the presence of mainly haematite (Fe_2O_3) and a minor proportion of magnetite (Fe_3O_4), pyrite (FeS_2), and traces of quartz (SiO_2).

3.2. Experimental procedures

Arsenic removal tests were performed by dissolving the pyrite ash wastes in alkaline solutions. The effects of leaching temperature (X_1) (60, 70, 85, 90, and 95°C), initial concentration of sodium hydroxide (NaOH) (X_2) (0.5, 1, 1.75, 2.5, and 3 M), and leaching time (X_3) (38, 120, 240, 360, and 440 min) on the extent of the removal of arsenic from pyrite ash solutions were investigated at five levels. The parameters and their levels in the experimental design were presented in Table 3. All experiments were carried out using 0.5% of solids in 300 mL of leach solutions, stirred at 400 rpm. After leaching and centrifugation, the residues were dried and sampled. The samples were then analyzed by ICP-MS.

4. Results and discussion

4.1. Solubility of different elements

In order to identify solubility of different elements by leaching, solid residue was obtained from the leaching test at which the highest arsenic extraction occurred. The leach residue used was obtained under the following leaching conditions: 3 M NaOH, 0.5% of solids, a reaction temperature of 80°C, and a leaching time of 4 h. There was practically a complete solubilization of As and partial solubilization of Pb, Al, Mo, and Cu, while Ni, Co, and Fe were concentrated almost entirely in the solid residue (Fig. 3 and Table 4).

4.2. Response analysis and interpretation

CCD with eight cube points, two central points in cube, and six axial points is given in Table 5. The actual and predicted levels of the variables for each of 16 experiments were calculated using the MINITAB as listed in Table 5. The leaching yield of As varied between 67 and 93%. *P* value was used to check the

Table 4
Chemical composition of As bearing ore and leach residue

Concentration	ppm									%	
Elements	As	Mo	Cu	Pb	Zn	Ni	Co	Mn	Bi	Fe	Al
As bearing ore	802.5	24.8	9,481	165	1,134	48	2,033	77.46	8.9	60.6	0.86
Leach residue	55	12	6,166	18	974	47.1	2,032	61	8	60.59	0.31

Table 5
Experimental design matrix and results

Run no.	Coded level of variables			Leaching yield of As (%)	
	X_1	X_2	X_3	Experimental	Predicted
1	−1	−1	−1	79	77.3
2	1	−1	−1	90	89.1
3	−1	1	−1	80	80.5
4	1	1	−1	91	90.7
5	−1	−1	1	78	78.4
6	1	−1	1	91	90.7
7	−1	1	1	80	81.1
8	1	1	1	90	91.8
9	−1.6818	0	0	67	69.9
10	1.6818	0	0	89	88.9
11	0	−1.6818	0	86	87.6
12	0	1.6818	0	93	91.2
13	0	0	−1.6818	84	85.5
14	0	0	1.6818	89	87.3
15	0	0	0	87	87.0
16	0	0	0	87	87.0

Table 6
Estimated regression coefficients for yield (%)

Term	Coef	SECoef	*T*	*P*
Constant	86.9662	1.3666	63.636	0
Temperature (℃)	6.0043	0.5245	11.447	0
NaOH concentration (M)	1.0817	0.5245	2.062	0.085
Time (min)	0.5425	0.5245	1.034	0.341
Temperature (℃) × Temperature (℃)	−3.1005	0.6368	−4.868	0.003
NaOH concentration (M) × NaOH concentration (M)	0.9654	0.6368	1.516	0.18
Time (min) × Time (min)	−0.095	0.6368	−0.15	0.886
Temperature (℃) × NaOH concentration (M)	−0.375	0.6853	−0.547	0.604
Temperature (℃) × Time (min)	0.125	0.6853	0.182	0.861
NaOH concentration (M) × Time (min)	0.125	0.6853	−0.182	0.861

Note: $S = 1.938$, $R^2 = 96.7\%$, R^2 (adj) = 91.8%.

Table 7
Analysis of variance for yield (%)

Source	DF	Seq SS	Adj SS	Adj MS	*F*	*P*
Regression	9	664.394	664.394	73.822	19.65	0.001
Linear	3	512.346	512.346	170.782	45.45	0
Square	3	150.673	150.673	50.224	13.37	0.005
Interaction	3	1.375	1.375	0.458	0.12	0.944
Residual error	6	22.544	22.544	3.757		
Lack of fit	5	22.544	22.544	4.509		
Pure error	1	0	0	0		
Total	15	686.937				

significance of each factor and factor interaction [21]. According to the *p*-value <0.05, the model is significant.

The response surface regression results gave the coefficient for all the terms, and each effect was estimated independently (Table 5). Table 6 shows that the variable with the largest effect on arsenic removal was the temperature effect, having a *p* value of 0.000 and temperature × temperature effect, with *p* values of 0.003. The accuracy and variability of the model [21] is calculated using R^2 which should be at least 0.8 [22]. The R^2 value was 0.967, which indicated a good agreement between experimental and predicted % leaching yields.

Table 7 shows the results of ANOVA (variance) analysis. The *p* value (0.001) for this model was less than 0.05 (Table 7), suggesting that the model is statistically significant. The analysis-of-variance table shows that the interaction between temperature, NaOH concentration, and leaching time was not statistically significant. The final equation in terms of coded factors was selected in Eq. (2) as follows,

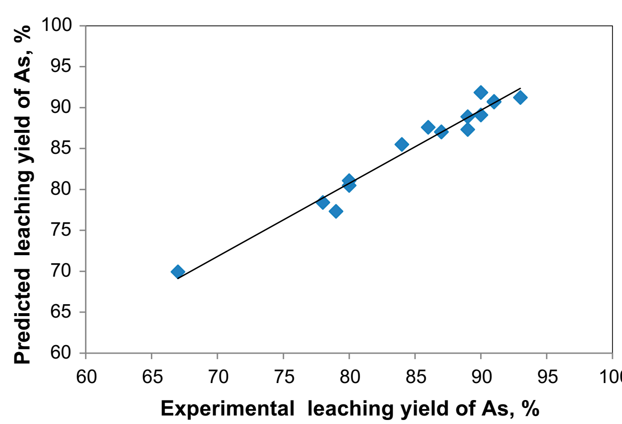

Fig. 4. Comparison model of prediction with the experimental data.

for As leaching yield:

$$Y = 86.99 + 6X_1 + 1.08X_2 + 0.54X_3 - 3.10X_1^2 + 0.96X_2^2 - 0.09X_3^2 - 0.37X_1X_2 + 0.12X_1X_3 - 0.12X_2X_3 \quad (2)$$

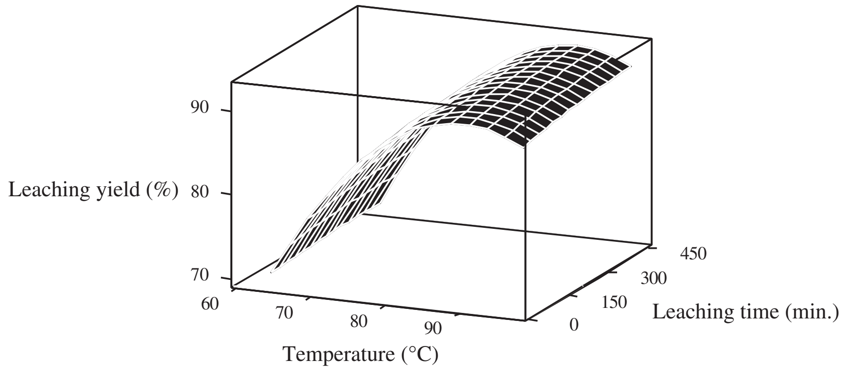

Fig. 5. A three-dimensional response surface map of temperature vs. leaching time on leaching yield at a NaOH concentration of 2.5 M.

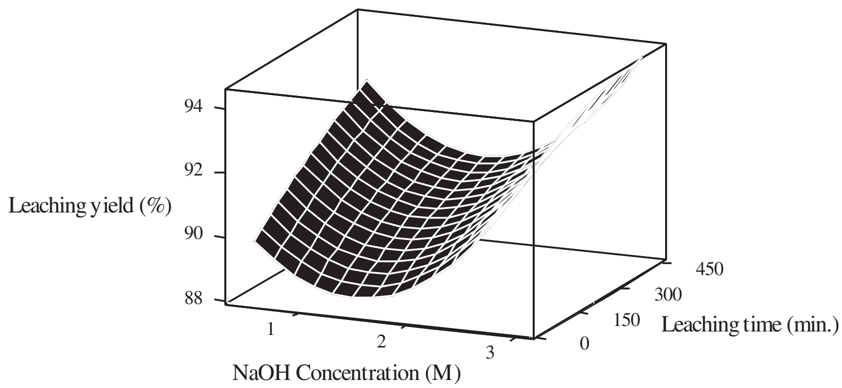

Fig. 6. A three-dimensional response surface map of NaOH concentration vs. leaching time on leaching yield at 90℃.

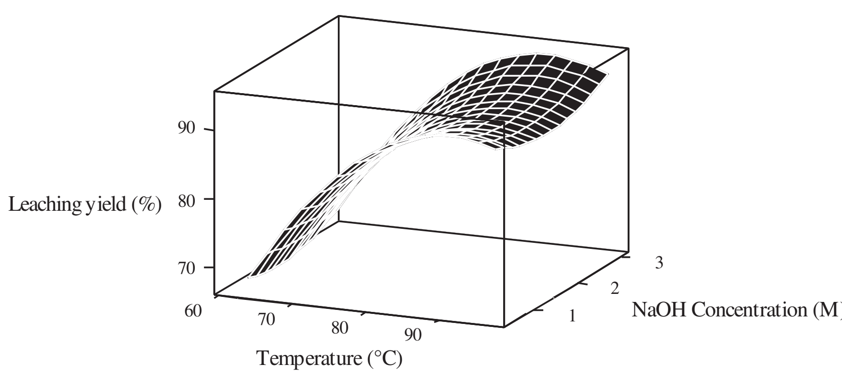

Fig. 7. A three-dimensional response surface map of NaOH concentration vs. temperature on leaching yield at a leaching time of 360 min.

The As leaching yield (Y) was expressed as a function of temperature (X_1), NaOH concentration (X_2), and leaching time (X_3) for coded units. The predicted values of yield (%) were obtained using Eq. (2).

4.3. Process optimization

Fig. 4 illustrates that the experimental responses correlated very well with the predicted values. Therefore, the models were considered adequate for the predictions and optimization of the process.

Table 8
Optimum leaching conditions and comparative results between predicted and experimental

Temperature ℃, X_1	NaOH concent. M, X_2	Time min, X_3	Leaching efficiency %	
			Predicted	Experimental
89.934	3.00	182.62	93.49	92.15

The effects of the three independent variables on the leaching yield using three-dimensional (3D) response surface plots for process optimization, constructed by MINITAB, are shown in Figs. 5–7.

As shown in Fig. 5, the highest leaching yield was obtained for high temperatures. An increase in temperature from 63 to 96℃ increased the leaching yield from 67 to 89%. Unlike the temperature effect, the leaching time had a negligible effect on the leaching yield (Fig. 5). Samuel and Sandstrom [23] recommended the selective leaching of arsenic from complex sulphide concentrate using alkaline solution and concluded that arsenic leaching was achieved at high temperatures. As a result, arsenic dissolution increased with increasing temperature. Fig. 6 shows that leaching yield increased with increasing NaOH concentration. NaOH concentration has little influence on the leaching yield. For example, it is possible to achieve high yield in a short period of leaching time with high levels of NaOH and high temperature.

The optimum leaching conditions were identified using the Design-Expert software to maximize the leaching efficiency (Table 8). As seen in Table 8, under optimum conditions, an average leaching efficiency of 92.15% was achieved for three experimental runs.

5. Conclusion

Pyrite ash contains hazardous heavy metals posing potential environmental risks for disposal. In this study, statistically designed experiments were performed to investigate the leaching of arsenic from pyrite ash using NaOH and three factors (i.e. leaching temperature, NaOH concentration, and leaching time) were taken into account. The proposed model equation using RSM agreed well with the experimental data, with a correlation coefficient (R^2) of 0.967. The results showed that the leaching temperature had a significant effect on the leaching yield (%), while other parameters exhibited little effect. The leaching yield of As varied between 67 and 93%. The optimum conditions for arsenic leaching from pyrite ash were identified as follows: NaOH concentration at 3 M, leaching temperature at 89℃, and leaching time of 182 min. Under these conditions, an average leaching yield of 92.15% was achieved from pyrite ash.

Acknowledgement

The authors would like to thank Karadeniz Technical University Scientific Research Fund (Project Kod No: 2013ARGEBD-9040) for the financial support of this work.

References

[1] İ. Alp, H. Deveci, E.Y. Yazıcı, T. Türk, Y.H. Süngün, Potential use of pyrite cinders as raw material in cement production: Results of industrial scale trial operations, J. Hazard. Mater. 166 (2009) 144–149.
[2] N. Tugrul, E.M. Derun, M. Piskin, Utilization of pyrite ash wastes by pelletization process, Powder Technol. 176 (2007) 72–76.
[3] N. Tugrul, E.M. Derun, M. Piskin, Effects of calcium hydroxide and calcium chloride addition to bentonite in iron ore pelletization, Waste Manage. Res. 24 (2006) 446–455.
[4] I. Alp, H. Deveci, H. Sungun, Utilization of flotation wastes of copper slag as raw material in cement production, J. Hazard. Mater. 159 (2008) 390–395.
[5] N. Borulu, T. Çalban, S. Kuşlu, S. Çolak, Pirit küllerinden yüksek fırına malzeme hazırlanması (Preparation of materials from pyrite ash to blast furnace), Tenth National Chemical Engineering Congress, Koç University, Istanbul, 3–6 September 2012.
[6] N. Tugrul, E.M. Derun, M. Piskin, S. Pişkin, Pelletzation of pyrite ash wastes for utilization in iron production industry, Sigma 3 (2005) 118–125.
[7] N. Tugrul, E.M. Derun, M. Piskin, Evaluation of pyrite ash wastes obtained by sulfuric acid production industry, Proceedings of the 8th International Conference on Environmental Science and Technol, Greece, 2003, pp. 918–925.
[8] A. Korkmaz, A. Horuz, Effects of EDTA on Fe–Mn–Zn contents released from pyrite ash and corn growth in pyrite ash applied peat media, J. Fac. Agric. 20 (2005) 11–14.
[9] M. Lim, G.C. Han, J.W. Ahn, K.S. You, H.S. Kim, Leachability of Arsenic and heavy metals from mine tailings of abandoned metal mines, Int. J. Environ. Res. Public Health 6 (2009) 2865–2879.
[10] H.S. Altundoğan, S. Altundoğan, F. Tümen, M. Bildik, Arsenic removal from aqueous solutions by adsorption on red mud, Waste Manage. 20 (2000) 761–767.
[11] Y. Li, Z. Liu, Q. Li, Z. Zhao, Z. Liu, L. Zeng, Removal of arsenic from Waelz zinc oxide using a mixed NaOH–Na_2S leach, Hydrometallurgy 108 (2011) 165–170.

[12] J.J. Ke, R.Y. Qiu, C.Y. Chen, Recovery of metal values from copper smelter flue dust, Hydrometallurgy 12 (1984) 217–224.
[13] M.H.V. Espinosa, Process for the removal of arsenic or arsenic compounds, United States Patent 3220796, Madrid, Spain, 1965.
[14] M. Leist, R.J. Casey, D. Caridi, The management of arsenic wastes: Problems and prospects, J. Hazard. Mater. 76 (2000) 125–138.
[15] Y. Li, Z. Liu, Q. Li, Z. Zhao, Z. Liu, L. Zeng, Removal of arsenic from arsenate complex contained in secondary zinc oxide, Hydrometallurgy 109 (2011) 237–244.
[16] A. Ito, T. Takachi, K. Kitada, J. Aizawa, T. Umita, Characteristics of arsenic elution from sewage sludge, Appl. Organomet. Chem. 15 (2001) 266–270.
[17] D.C. Montgomery, Design and Analysis of Experiments, Wiley, New York, NY, 2001.
[18] G.E.P. Box, K.B. Wilson, On the experimental attainment of optimum conditions, J. R. Stat. Soc. Ser. B: Stat. Methodol. 13 (1951) 1–45.
[19] J. Liu, S. Wen, D. Liu, M. Lv, Response surface methodology for optimization of copper leaching from a low-grade flotation middling, J. Miner. Metall. Process 28 (2011) 139–145.
[20] C.Y. Khor, M.Z. Abdullah, Optimization of IC encapsulation considering fluid/structure interaction using response surface methodology, Simul. Model. Pract. Theory 29 (2012) 109–122.
[21] T.K. Trinh, L.S. Kang, Application of response surface method as an experimental design to optimize coagulation tests, Environ. Eng. Res. 15 (2010) 63–70.
[22] K.D. Yang, X.J. Ye, J. Su, H.F. Su, Y.F. Long, X.Y. Lü, Y.X. Wen, Response surface optimization of process parameters for reduction roasting of low-grade pyrolusite by bagasse, Trans. Nonferrous Met. Soc. China 23 (2013) 548–555.
[23] A.A. Samuel, A. Sandstrom, Selective leaching of arsenic and antimony from a tetrahedrite rich complex sulphide concentrate using alkaline sulphide solution, Miner. Eng. 23 (2010) 1227–1236.